20169063

Reduction in Radiation Noise Level for Inductive Power Transfer System with Spread Spectrum

Keisuke Kusaka [1)] Kent Inoue [2)] Jun-ichi Itoh [3)]

1) Nagaoka University of Technology, Energy and Environment Science

1603-1 Kamitomioka, Nagaoka, Niigata, 940-2188, Japan (E-mail: kusaka@stn.nagaokaut.ac.jp)

2) Nagaoka University of Technology, Electrical, Electronics and Information Engineering

1603-1 Kamitomioka, Nagaoka, Niigata, 940-2188, Japan (E-mail: k_inoue@stn.nagaokaut.ac.jp)

3) Nagaoka University of Technology, Electrical, Electronics and Information Engineering

1603-1 Kamitomioka, Nagaoka, Niigata, 940-2188, Japan (E-mail: itoh@vos.nagaokaut.ac.jp)

Presented at the EVTeC and APE Japan on May 26, 2016

ABSTRACT: Reduction methods in radiation noise of inductive power transfer (IPT) systems for electrical vehicles (EVs) are proposed. In the IPT system for EVs, noise reduction technologies are required because radiation noise from the IPT system have to be suppressed to satisfy the standards. By changing the output frequency of the inverter, the radiation noise from the transmission coils is spread in a frequency domain. From the experimental results, the harmonics components around fundamental frequency are suppressed by 33.1% by using the proposed method in comparison with the system using a constant frequency.

KEY WORDS: inductive power transfer, radiation noise, spread spectrum, Stationary Wireless Power Transfer (E5)

1. INTRODUCTION

In recent years, IPT systems for EVs or plug-in hybrid electrical vehicles (PHEVs) are actively studied and developed [(1-6)]. The IPT system transmits power using a magnetic coupling between a primary coil and a secondary coil. The fundamental principle of the IPT system is as same as a transformer. However it is characterized that the coupling between the primary coil and the secondary coil are weak such as 0.1–0.3. The practical realization of the IPT system is highly expected because the IPT systems are capable to improve a usability of the EVs and PH EVs.

In order to put the IPT system into practical use, radiated electromagnetic noise has to be suppressed to satisfy the standards[(7-8)], which are published by CISPR are well-known standards, because the IPT system never affects any radio communication systems, or electronic equipment. As a conventional method, a suppression method using a filter circuit has been proposed. The low pass filter is used at the input stage of the primary coil. The filter circuit suppresses the harmonics components of the current on the primary coil. However, the fundamental components of the transmission coil cannot be suppressed. Moreover the larger power loss on the filter circuit occurs since the cut-off frequency of the filter circuit is closed to the fundamental frequency. References (9-12) have proposed the suppression methods using a magnetic shield and a metal shield. The transmission coils are surrounded by the plates made by magnetic material or metal. The radiation noise can be suppressed because these shields change a magnetic flux to an eddy current. However the eddy current increases the power loss of the IPT system. Moreover, the additional magnetic or metal shields cause an increase of cost.

Incidentally, a spread spectrum method is widely used in a motor drive system with a PWM inverter [(13)]. In the part of the motor drive system, the carrier frequency of the PWM inverter is constantly changed during the operation for the purpose of a reducing acoustic noise. By changing the carrier frequency, the frequency components of the acoustic noise caused by vibrations of windings of the motor is spread in a frequency domain [(13)].

In this paper, two reduction methods on the radiation noise using the spread spectrum are proposed. In the proposed system, the output frequency of the voltage-source inverter is changed within 80 kHz to 90 kHz at each output period. The proposed method does not require additional components. Moreover, the effect on the efficiency is small. In the chapter 3, two reduction methods are proposed. The proposed methods varied the output frequency of the voltage-source inverter. In the first proposed method, the frequency is continuously changed. In contrast, the frequency is changed in random in the second proposed method. Then the proposed methods are demonstrated using a scale model of the IPT system with an output power of 200 W in the chapter 4. In the chapter 5, the proposed method is implemented into the prototype with an output power of 3 kW. Finally, the effect on the system efficiency is evaluated.

2. ALLOWABLE RADIATION NOISE LEVEL IN JAPAN

Fig. 1 shows the standards of the radiation noise in Japan for IPT systems. Note that, the standards are still under discussion for the standardization. In Japan, a use of a frequency range from 79 kHz to 90 kHz is considered for the IPT system of EVs or PHEVs. This standard is basically conformed to the CISPR11 (14). The difference between the CISPR11 and the standards is an allowable limit on the transmission frequency and its low-order harmonics. The allowable limits of the radiation noise within 79 kHz to 90 kHz will be mitigated to 68.4 dBμA/m. Moreover, the allowable limits on low order harmonics components will be mitigated by 10 dB. Note that, CISPR11 requires measuring the noise by a quasi-peak detection method. In order to satisfy the standards, the frequency components of the radiation noise should be suppressed not only the fundamental component but also the low-order harmonics component.

3. PROPOSED NOISE REDUCTION METHODS

The radiation noise is mainly caused by the current, which flows in the transmission coils. In the conventional system, the output frequency of the inverter is generally constant. Thus, the radiation noise contains the large output frequency components and its low-order harmonic components.

In this paper, the radiation noise is spread in a frequency domain by changing the output frequency of the voltage-source inverter in two manners. The output frequency is varied within 80 kHz to 90 kHz. In the one of the proposed methods, the output frequency is continuously changed. Another method changes the switching frequency of the inverter in random.

Fig. 2 shows the schemes of frequency changing. Fig. 2 (a) is the frequency changing pattern of the proposed method I. The output frequency of the inverter is discretely chosen according to the triangular waveform. The frequency of an output frequency changing is 2 kHz. Each frequency step is 650 Hz. Fig. 2 (b) shows the probability distribution of the output frequency when the proposed method II is used. In this method, the output frequency of the voltage-source inverter is changed in random. The output frequency is chosen according to a pseudo random number. Thus the probability distribution of the output frequency is approximately even. The pseudo random number is generated using a maximal length sequence (M-sequence) in the DSP. Note that, different pseudo random number generation methods can be used. However the generation method using an M-sequence is chosen in this paper because a complex generation method of a pseudo random number is not suitable for an implementation to the DSP.

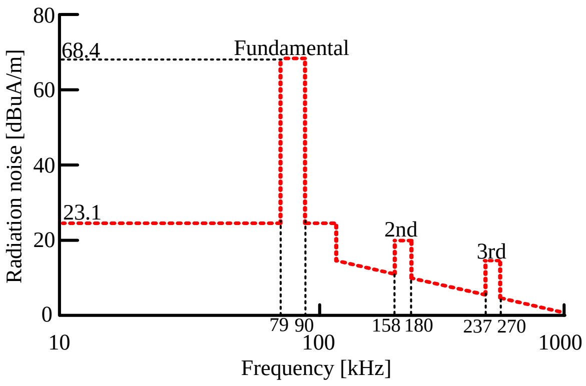

Fig. 1. Allowable Limits on Radiation Noise of IPT System for EVs in Japan (under discussion).

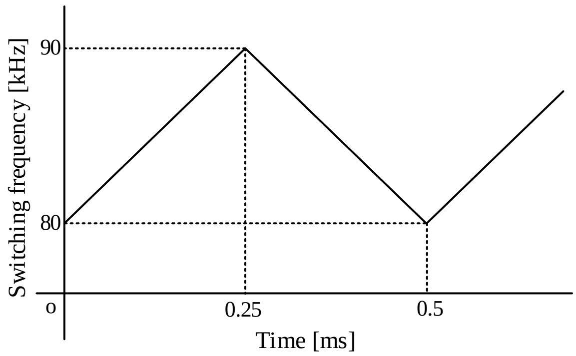

(a) Proposed method I: The output frequency is varied according to the triangle wave.

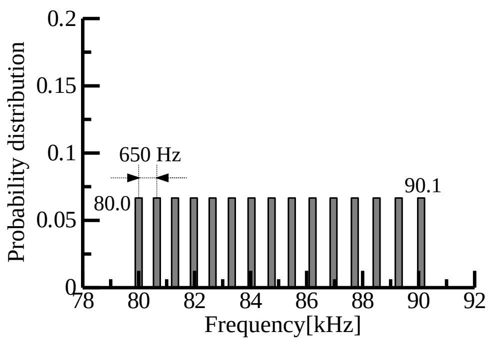

(b) Proposed method II: The frequency is chosen in random.

Fig. 2 Frequency Changing Pattern of Proposed Methods.

Fig. 3 shows the generation method of pseudo random numbers based on an M-sequence. An M-sequence random number is generated by (1).

$$X_Z = X_{Z-p} \oplus X_{Z-q} \qquad (1)$$

where X_{z-p} and X_{z-q} are the present value X_Z delayed by p period and q period, respectively ($p > q$). In this paper, $p = 7$, $q = 1$ are used. Moreover, the number of bits of pseudo random number is seven.

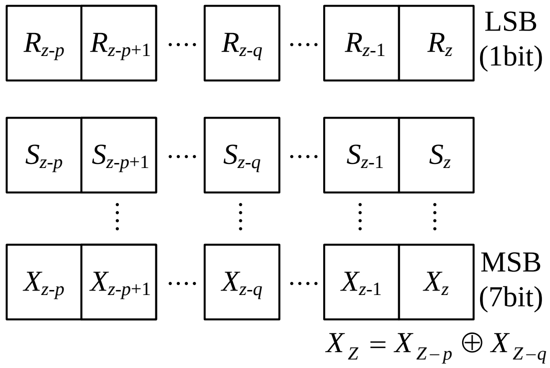

Fig. 3. Generation Method of Pseudo Random Numbers Base on a Maximal Length Sequence.

4. EXPERIMENTS WITH SCALE MODEL

In this chapter, the conventional method and the proposed methods are experimentally evaluated using a scale model.

4.1. Experimental Setup

Fig. 4 and Table 1 show the circuit configuration of the prototype and the specifications, respectively. The proposed methods are tested with a scale model. In the scale model, the output power is reduced from 3 kW to 200 W for simplicity. The series-series (S/S) compensation method is used in order to cancel out the leakage inductance [15]. Beside, silicon-carbide (SiC) MOSFETs and SiC diodes are used as switching devices. The output frequency of the primary inverter is decided in the DSP.

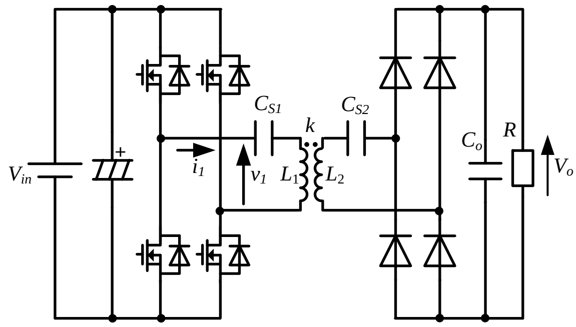

Fig. 4. System Configuration.

Table 1. Specifications of Prototype (Scale model).

	Symbol	Value
Input DC voltage	V_{in}	100 V
Coupling coefficient	k	0.35
Primary inductance	L_1	176 uH
Secondary inductance	L_2	180 uH
Primary capacitance	C_{S1}	19.6 nF
Secondary capacitance	C_{S2}	19.4 nF
Transmission distance	l	9 mm

4.2. Operation waveforms

Fig. 5 shows the experimental results of the prototype. Fig. 5 (a) is the waveforms with a constant-frequency. Fig. 5 (b) is the waveforms with a proposed method I: the output frequency is varied according to the Fig. 2 (a). Fig. 5 (c) is the waveforms with the proposed method II: the output frequency is changed in random. In Fig. 5 (b) and (c), the output frequency of the inverter is changed within 80 kHz to 90 kHz in every periods according to pseudo random numbers. Due to the difference between the resonance frequency and the amplitude of the primary current i_1 is changed.

Fig. 6 shows the harmonics components of the primary current i_1. Fig. 6 (a) is the result with the conventional method. Fig. 6 (b) and (c) are the results with the proposed methods. In this paper, the harmonics components of the primary current are evaluated instead of the radiation noise because the radiation noise from a loop coil is proportional to the amplitude of current. When the conventional method is used, the current with an output frequency and low-order harmonics components are sharp. In contrast, the proposed method I: the switching frequency is varied according to triangle wave, and the proposed method II: the switching frequency is varied in random, suppress the harmonics components around the fundamental frequency of 85 kHz by 37.2% and 57.0% in comparison with the conventional method, which operates the inverter at constant frequency. In same manner, the low-order harmonic components are suppressed in comparison with the conventional method. From the experiments with scale model, it is clear that the proposed method, which varied the output frequency in random, is effective to suppress the radiation noise. Thus the proposed method is implemented into the second prototype, which has an output power of 3 kW.

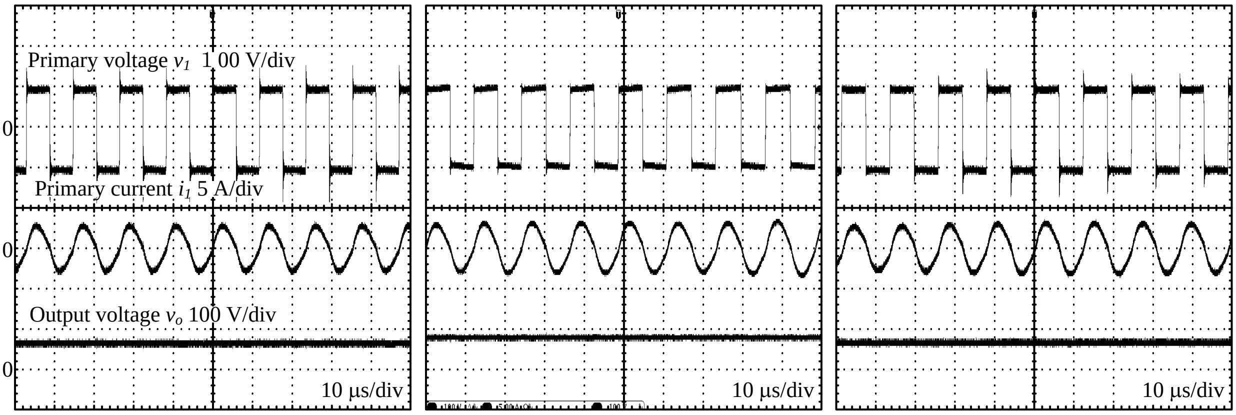

(a) Constant frequency. (b) Varied frequency according to triangle wave. (c) Varied frequency in random.

Fig. 5. Operation waveforms with scale model. The output power is 200 W.

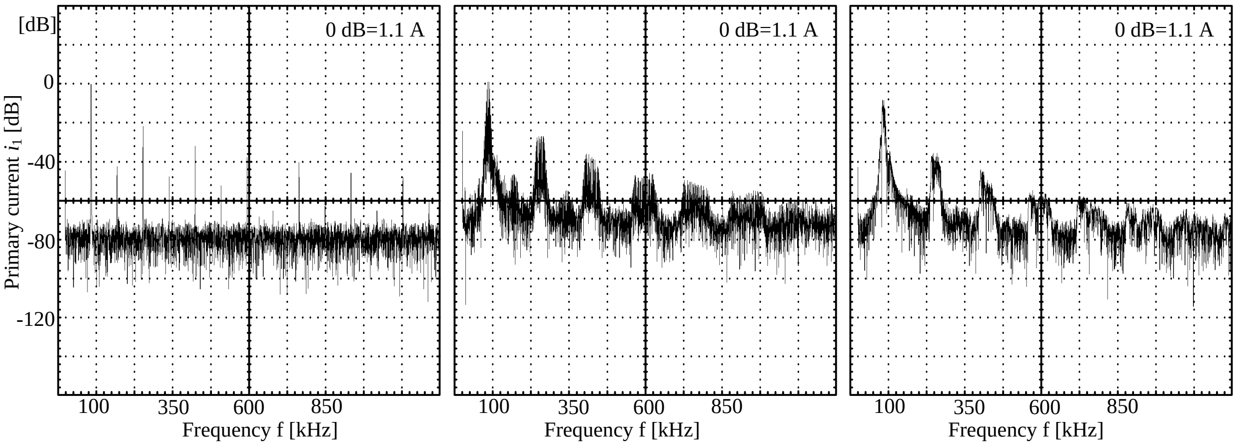

(a) Constant frequency (b) Varied frequency according to triangle wave (c) Varied frequency in random

Fig. 6. Harmonics Analysis of Primary Current.

5. EXPERIMENTS WITH 3-KW PROTOTYPE

In this chapter, the proposed method is demonstrated with the 3-kW prototype. The output frequency of the inverter is varied in random.

5.1. Experimental Setup

Fig. 7 and Table 2 show the transmission coils, which are used in the experiments and specifications of the prototype, respectively. Solenoid coils are used as the transmission coils. The transmission distance is 150 mm.

5.2. Operation Waveforms

Fig. 8 shows the operation waveforms. Fig. 8 (a) is the waveforms with a constant output frequency of 85.1 kHz. Fig. 8 (b) is the waveforms with the proposed method. The output frequency of the voltage source inverter is varied within 80 kHz to 90 kHz in random. In both of the operation waveforms, the output power is 3 kW. When the proposed method is applied, the amplitude of the output current of the inverter is varied due to the

Fig. 7. Transmission Coils for 3-kW Prototype.

Table 2. Specifications of Prototype.

	Symbol	Value
Input DC voltage	V_{in}	420 V
Coupling coefficient	k	0.2
Primary inductance	L_1	392 uH
Secondary inductance	L_2	401 uH
Primary capacitance	C_{S1}	8.96 nF
Secondary capacitance	C_{S2}	8.78 nF
Transmission distance	l	150 mm
MOSFETs	ROHM: SCH2080KEC	
Diodes	ROHM: SCS220AE	

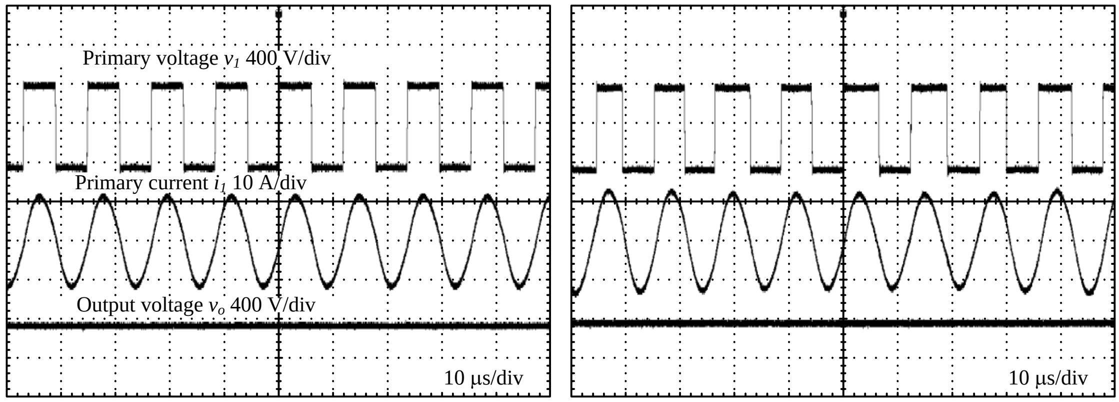

(a) Constant frequency (b) Varied frequency in random

Fig. 8. Operation Waveforms with 3-kW Prototype.

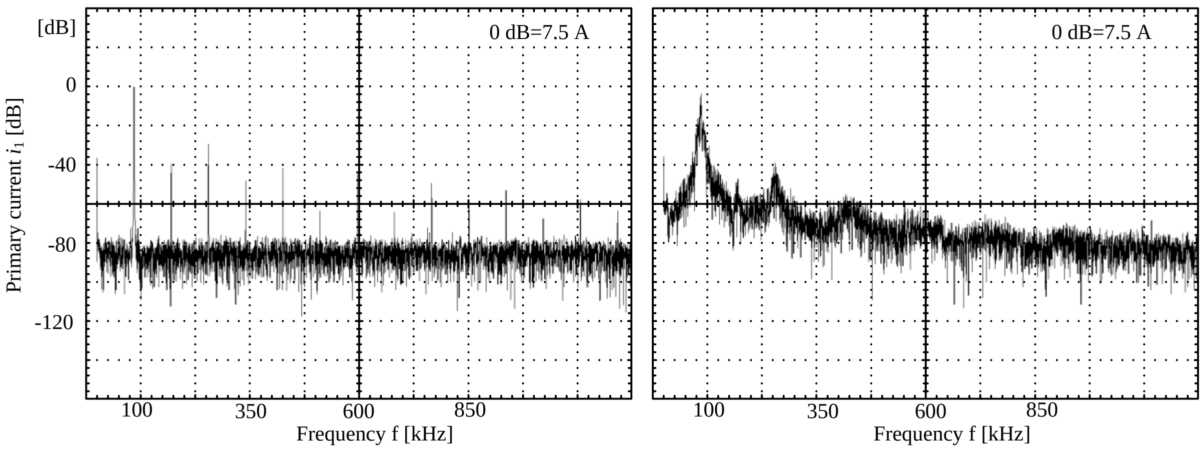

(a) Constant frequency. (b) Varied frequency in random.

Fig. 9. Harmonics Analysis of Primary Current.

difference between the resonance frequency and the inverter output frequency.

Fig. 9 shows the harmonics components of the primary current i_1. Fig. 9 (a) and (b) are the result without the proposed method and the result with the proposed method. In this paper, the harmonics components of the primary current is evaluated instead of the radiation noise because the radiation noise from a loop coil is proportional to the amplitude of a current. The components around the fundamental frequency are suppressed by 33.1% by applying the proposed method. In same manner, the low-order harmonic components are suppressed in comparison with the operation without the proposed method.

5.3. Efficiency Comparison

Fig. 10 shows the DC-to-DC efficiency characteristics. Note that the efficiency is defined as the ratio of the output DC power to the input DC power. Both curve show similar characteristic. The maximum efficiency is 94.9% at an output power of 3.0 kW when the inverter is operated at constant frequency. In contrast, the maximum efficiency is 94.1% at an output power of 3.0 kW

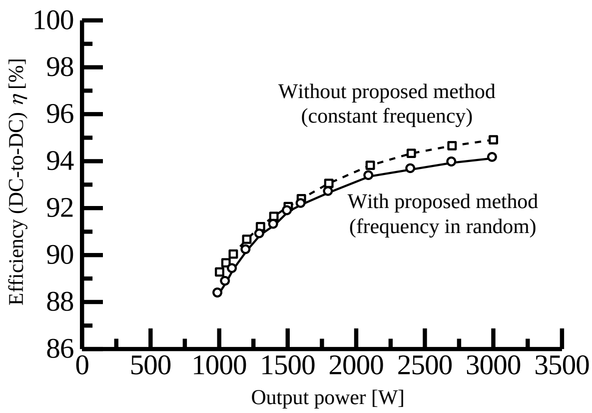

Fig. 10. Efficiency characteristic.

when the proposed method is used. The decrease of efficiency is due to the difference of the resonant frequency and the output frequency of the inverter. However, the decrease in efficiency is 0.84%. The effect of the spread spectrum on the efficiency is enough small to be ignored.

6. CONCLUSION

In this paper, the reduction methods in a radiation noise of the IPT systems for EVs are proposed. In the IPT system for EVs, noise reduction technologies are required because the radiation noise from the IPT system has to be suppressed to satisfy the standards. By changing the output frequency of the inverter, the radiation noise from the transmission coils is spread in a frequency domain. In this paper, two reduction methods based on the spread spectrum are proposed. One of the proposed methods varies the output frequency of the inverter according to the triangle wave. Another varies the output frequency in random. First, the conventional method and the proposed methods are experimentally evaluated with a scale model at an output power of 200 W. The results shows that the reduction rate of the harmonics components of the second proposed method, which varies the output frequency in random, is larger than the first proposed method, which varies the frequency according to triangle wave. Then the second method is implemented into the 3-kW prototype. From the experimental results, the harmonics components around fundamental frequency are suppressed by 33.1% by using the proposed method in comparison with the system using a constant frequency. In addition, the decrease of the transmission efficiency at the rated power is 0.84%.

REFERENCES

(1) R. Chen, C. Zheng, Z. U. Zahid, E. Faraci, M. Senesky, D. Anderson, G. lisi: Analysis and Parameters Optimization of a Contactless IPT System for EV Charger, IEEE Applied Power Electronics Conference and Exposition 12th, Vol. , No. , pp. 1654-1661 (2014)

(2) H. H. Wu, A. gilchrist, K. D. Sealy, D. Bronson: A High Efficiency 5 kW Inductive Charger for EVs Using Dual Side Control, IEEE Trans. On Industrial Informatics, Vol. 8, No. 3, pp. 585-595 (2012)

(3) M. Budhia, J. T. Boys, G. A. Covic, C. Huang: Development of a Single-Sided Flux Magnetic Coupler for Electric Vehicle IPT Charging Systems, IEEE Trans. On Industrial Electronics, Vol. 60, No. 1, pp. 318-328 (2013)

(4) R. Haldi, K. Schenk: A 3.5 kW Wireless Charger for Electric Vehicles with Ultra High Efficiency, IEEE Energy Conversion Congress & Expo 2014, Vol. , No. , pp. 668-674 (2014)

(5) M. Jo, Y. Sato, Y. Kaneko, S. Abe: Methods for Reducing Leakage Electric Field of a Wireless Power Transfer System for Electric Vehicles, IEEE Energy Conversion Congress & Expo 2014, Vol. , No. , pp. 1762-1769 (2014)

(6) H. Takanashi, Y. Sato, Y. Kaneko, S. Abe, T. Yasuda: A Large Air Gap 3 kW Wireless Power Transfer System for Electric Vehicles, IEEE Energy Conversion Congress & Expo 2012, Vol. , No. , pp. 269-274 (2012)

(7) H. Shoki: Trends of Wireless Power Transmission Technologies and Approaches for Commercialization, IEICE Technical Report, No. WPT2010-07, pp. 19-24 (2010)

(8) J. Kim, H. Kim, M. Kim, S. Ahn, J. Kim, J. Kim: Analysis of EMF Noise from the Receiving Coil Topologies for Wireless Power Transfer, Asia-Pacific Symposium on Electromagnetic Compatibility (APEMC) 2012 , pp.645-648 (2012)

(9) M. Jo, Y. Sato, Y. Kaneko, S. Abe: “Methods for Reducing Leakage Electric Field of a Wireless Power Transfer System for Electric Vehicles”, ECCE US, pp.1762-1769 (2014)

(10) H. Kim, J. Cho, S. Ahn, J. Kim, J. Kim: “Suppression of Leakage Magnetic Field from a Wireless Power Transfer System using Ferrimagnetic Material and Metallic Shielding”, IEEE International Symposium on EMC, 978-1-4673-2061-0, pp.640-645 (2012)

(11) T. Campi, S. Cruciani, M. Feliziani: “Magnetic Shielding of Wireless Power Transfer Systems”, IEEE International Symposium on EMC, 15A-H1, pp.422-425 (2014)

(12) K. Maikawa, K. Imai, Y. Minagawa, M. Arimitsu, H. Iwao: “Magnetic Field Reduction Technology of Wireless Charging System”, in Proceedings, Society of Automotive Engineers of Japan 2013, No. 110-13 (2013)

(13) J. T. Boys, P. G. Handley: Spread spectrum switching: low noise modulation technique for PWM inverter drives, IEE Proceedings B (Electric Power Applications), Vol.139, No.3, pp. 252-260 (1992)

(14) International Electrotechnical Commission: CISPR 11, Industrial, scientific and medical equipment – Radio-frequency disturbance characteristics – Limits and methods of measurement, Edition 5.1 (2015)

(15) Y. H. Sohn, B. H. Choi, E. S. Lee, G. C. Lim, G. Cho, C. T. Rim: General Unified Analyses of Two-Capacitor Inductive Power Transfer Systems: Equivalence of Current-Source SS and SP Compensations, IEEE Trans. On Power Electronics, Vol. 30, No. 11, pp. 6030-6045 (2015)